

Properties of Polyelectrolyte Templates Generated by Dip-Pen Nanolithography and Microcontact Printing

Dorjderem Nyamjav[†] and Albena Ivanisevic^{*‡}

Departments of Physics, Biomedical Engineering, and Chemistry, Purdue University, West Lafayette, Indiana 47907

Received May 24, 2004

Revised Manuscript Received October 19, 2004

The development of unconventional methods to pattern various surfaces on the micrometer and nanometer scales is important for a variety of applications such as optoelectronic devices, biomaterials, and tissue engineering.¹ For example, a number of soft lithography approaches exist (i.e., replica molding, embossing, and microcontact printing) to fabricate large arrays of self-assembled monolayers on different types of surfaces.² In addition, researchers have developed scanning probe methods that offer more flexibility to pattern nonplanar architectures with various (bio)molecules.^{3–5} Recently, the need for materials' surfaces with the following characteristics have been recognized:^{6,7} (i) tunable chemical functionality and spatial resolution; (ii) control over placement on the solid surface; and (iii) flexibility over the design of the topographical and chemical architecture. Such surfaces present an ideal test bed to study fundamental questions in areas such as cell adhesion where researchers are trying to determine and compare the importance of the local topography vs chemical composition.^{8–10} Therefore, the advancement of methods that provide control over the micron and nanoscale organization without compromising the control over the chemical architecture is needed. In particular, the usage of polyelectrolytes to accomplish this task is attractive as they offer the ability to adjust important parameters such as thickness, roughness, and availability of reactive and/or inert functional groups.^{11,12}

Previous lithography work by Hammond and co-workers has mostly focused on using microcontact printing on surfaces modified with either thiols or polyelectrolyte multilayers.^{13–18} In addition, Lvov et al. have shown that polyelectrolyte films can be placed selectively onto microfabricated silicon surfaces.^{19–21}

In this communication we fabricate a template composed of two types of polyelectrolyte features, one generated by dip-pen nanolithography (DPN)²² and another generated by microcontact printing.¹ We compare and contrast the properties of both types of features on the same surface and test them in assembly strategies. The experiments we performed allowed us to observe that the surface properties on the DPN and microcontact printed patterns are different. The variations in the surface properties of the two lithographic patterns are directly related to the results one obtains when the two types of patterns are used in directed assembly experiments. Taken in sum, the methodology we present permits the direct comparison of the lithographic patterns in terms of their size, homogeneity, adhesion, and recognition properties.

The overall fabrication process was initiated by generating features with the atomic force microscope (AFM) tip via DPN. In this approach, the tip is coated with ink molecules and brought into contact with the surface.²² The water meniscus that forms between the tip and the surface is used to transport molecules to a desired location on the substrate. All the DPN experiments were performed using Multi-Mode SPM from Digital Instruments, equipped with a Nanoscope software system. All the data were collected under ambient conditions, where the temperature range was 20–22 °C and the humidity was between 21 and 40%. The "V" shaped triangular contact and single beam shaped tapping mode tips (Veeco Instruments) had spring constants of 0.05 N/m and 42 N/m, respectively. AFM contact tips that were used for lithography experiments were coated by dipping them into a solution of PAH (poly(allylamine) hydrochloride, 2 mg in 1 mL of 5 mM NaCl) for 2–5 s. In a typical experiment, a tip coated with PAH was brought into contact with the surface of the freshly cleaned SiO_x substrate. The transfer process involves PAH diffusing onto the surface via capillary action once the tip contacts the surface. Frictional images, collected with a coated tip, showed that PAH features exhibit a lower lateral signal which can be attributed to repulsive electrostatic interactions between

* Corresponding author. E-mail: albena@purdue.edu.

[†] Department of Physics.

[‡] Departments of Biomedical Engineering and Chemistry.

(1) Gates, B.; Yin, Y.; Xia, Y. *Chem. Mater.* **1999**, *11*, 2827–2836.

(2) Gates, B. D.; Xu, Q.; Love, J. C.; Wolfe, D. B.; Whitesides, G. M. *Annu. Rev. Mater. Res.* **2004**, *34*, 339–372.

(3) Liu, G. Y.; Xu, S.; Qian, Y. *Acc. Chem. Res.* **2000**, *33*, 457–466.

(4) Kramer, S.; Fuieler, R. R.; Gorman, C. B. *Chem. Rev.* **2003**, *103*, 4367–4418.

(5) Ginger, D. S.; Zhang, H.; Mirkin, C. A. *Angew. Chem., Int. Ed.* **2004**, *43*, 30–45.

(6) Gleason, N. J.; Nodes, C. J.; Higham, E. M.; Guckert, N.; Aksay, I. A.; Schwarzbauer, J. E.; Carbeck, J. D. *Langmuir* **2003**, *19*, 513–518.

(7) Roth, E. A.; Xu, T.; Das, M.; Gregory, C.; Hickman, J. J.; Boland, T. *Biomaterials* **2004**, *25*, 3707–3715.

(8) Zhu, X.; Chen, J.; Scheideler, L.; Reichl, R.; Geis-Gerstorfer, J. *Biomaterials* **2004**, *25*, 4087–4103.

(9) Yousaf, M. N.; Houseman, B. T.; Mrksich, M. *Angew. Chem., Int. Ed.* **2001**, *40*, 1093–1096.

(10) Anselme, K.; Linez, P.; Bigerelle, M.; Maguer, D. L.; Maguer, A. L.; Hardouin, P.; Hildebrand, H. F.; Iost, A.; Leroy, J. M. *Biomaterials* **2000**, *21*, 1567–1577.

(11) Mendelsohn, J. D.; Yang, S. Y.; Hiller, J. A.; Hochbaum, A. I.; Rubner, M. F. *Biomacromolecules* **2003**, *4*, 96–106.

(12) Berg, M. C.; Yang, S. Y.; Hammond, P. T.; Rubner, M. F. *Langmuir* **2004**, *20* (4), 1362–1368.

(13) Jiang, X.; Hammond, P. T. *Langmuir* **2000**, *16*, 8501–8509.

(14) Jiang, X.; Ortiz, C.; Hammond, P. T. *Langmuir* **2002**, *18*, 1131–1143.

(15) Jiang, X.; Zheng, H.; Gourdin, S.; Hammond, P. T. *Langmuir* **2002**, *18*, 2607–2615.

(16) Lee, I.; Zheng, H.; Rubner, M. F.; Hammond, P. T. *Adv. Mater.* **2002**, *14*, 572–577.

(17) Zheng, H.; Lee, I.; Rubner, M. F.; Hammond, P. T. *Adv. Mater.* **2002**, *14*, 569–572.

(18) Lee, I.; Ahn, J. S.; Hendricks, T. R.; Rubner, M. F.; Hammond, P. T. *Langmuir* **2004**, *20*, 2478–2483.

(19) Hua, F.; Cui, T.; Lvov, Y. *Langmuir* **2002**, *18*, 6712–6715.

(20) Hua, F.; Shi, J.; Lvov, Y.; Cui, T. *Nano Lett.* **2002**, *2*, 1219–1222.

(21) Hua, F.; Cui, T.; Lvov, Y. M. *Nano Lett.* **2004**, *4*, 823–825.

(22) Piner, R. D.; Zhu, J.; Xu, F.; Hong, S.; Mirkin, C. A. *Science* **1999**, *283*, 661–663.

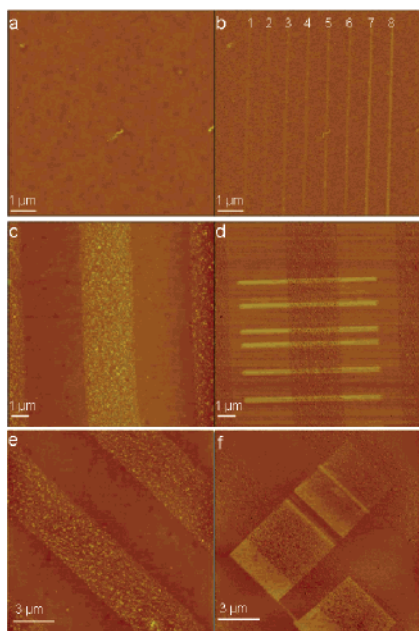


Figure 1. Patterns of PAH generated on a SiO_x surface. Parts (a) and (b) represent height and phase images, respectively, collected in TMAFM after the DPN procedure, as described in the text. These TMAFM images were acquired simultaneously with a scan size of $10 \times 10 \mu\text{m}^2$ and a frequency of 1.97 Hz. The height scale in (a) is 30 nm and in (b) is 10° of phase lag. Parts (c) and (d) represent height and phase images, respectively, collected in TMAFM after the DPN and microcontact printing procedures, as described in the text. These TMAFM images were acquired simultaneously with a scan size of $15 \times 15 \mu\text{m}^2$ and a frequency of 1.97 Hz. The height scale in (c) is 20 nm and in (d) is 20° of phase lag. Parts (e) and (f) represent height and phase images, respectively, collected in TMAFM after the DPN and microcontact printing procedures, as described in the text. These TMAFM images were acquired simultaneously with a scan size of $15 \times 15 \mu\text{m}^2$ and a frequency of 1.97 Hz. The height scale in (e) is 25 nm and in (f) is 20° of phase lag.

the tip and the deposited “ink”. In addition, we have verified the delivery of PAH to the surface via the DPN technique through X-ray photoelectron spectroscopy (XPS).²³ Furthermore, for this study we verified by XPS that the chemical composition of the DPN-generated structures is the same as the structures we generated by microcontact printing. However, XPS does not allow us to map the mechanical properties of the templates. To gain further insight into the morphology and composition of the features we utilized tapping mode AFM (TMAFM). The patterned substrate was washed with DI water and dried under nitrogen to remove excess, loosely bound polyelectrolytes. The washed surfaces were imaged by TMAFM, Figure 1A and B, to avoid damage to the soft structures on the surface.

TMAFM images allowed us to evaluate the results of the patterning primarily through phase contrast changes. The height image, Figure 1A, shows no appreciable differences across the entire area examined. However, in Figure 1B one can distinguish 8 different lines with $1\text{-}\mu\text{m}$ spacing. Studies have shown that in this imaging mode the phase image provides more contrast than the height image and can be sensitive to properties such as viscoelasticity, stiffness, and chemical composition.²⁴

Lines 1–8 were fabricated with different tip speeds. Lines 1 and 2, 3 and 4, 5 and 6, and 7 and 8 were written with tip speeds of $20 \mu\text{m/s}$ for 10 s, $20 \mu\text{m/s}$ for 30 s, $20 \mu\text{m/s}$ for 60 s, and $40 \mu\text{m/s}$ for 60 s, respectively. The scan size during the fabrication was $10 \mu\text{m}$ and the aspect ratio was 1:256. Since the aspect ratio of the scan size is 1:256 the tip goes over the same line with a length of $10 \mu\text{m}$ a number of times depending on the time spent to scan over it with a specific speed. The phase image suggests that the properties of the polyelectrolyte lines deposited during the DPN process are subject to the tip speed employed during writing as well as the number of times the tip repeatedly scanned over the same line. In principle, phase changes are very sensitive to parameters such as tapping force level (lighter or harder tapping), AFM probe shape, and anomalous topographical changes.²⁵ Therefore, matching phase changes with specific properties (e.g., chemical or mechanical properties) requires a comprehensive study that includes varying a number of parameters in order to attribute differences in phase contrast.²⁶ However, in this case we can use one phase image to compare the chemical properties of the different lines relative to one another since they are located on the same surface. In our experiments, the different lines can be imaged under the same conditions with any given tip. The phase changes across the image are due to chemical heterogeneity on the templated surface. At the same time the phase contrast within a single patterned line is at a consistent level which suggests that the individual DPN lines are chemically homogeneous. The amount of material deposited during the DPN process is not enough to produce a detectable height change, therefore the changes in surface topography that can influence the phase image are very small.

Another lithographic approach that has been used extensively to pattern polyelectrolytes is microcontact printing.^{13–18} We placed features generated by both methods on the same surface to better compare and contrast the properties of the structures generated by DPN. We initiated the process by cleaning the SiO_x surface, patterning lines by DPN (see above), and then stamping PAH on the same surface using a protocol reported by Lee et al.¹⁸ We show the results of this process, after the surface has been washed numerous times with water, in Figure 1C–F. The “ink” solution in both lithographic strategies was 2 mg of PAH in 1 mL of 0.5 M NaCl. The vertical stripes generated by microcontact printing are evident in both the height and the phase images. The DPN patterns (the six horizontal lines) are visible only in the phase image. The same trend is observed with the larger DPN structures, Figure 1F. In addition, one can clearly see the DPN patterns even in areas where the stamped stripes overlap them. Since the same type of ink was used for the two types of structures one is compelled to assign the bright and dark contrasts to hard or soft structures. However, this assignment is not straightforward and different studies have made variable conclusions.^{27–29}

(24) Raghavan, D.; Gu, X.; Nguyen, T.; VanLandingham, M.; Karim, A. *Macromolecules* **2000**, *33*, 2573–2583.

(25) Raghavan, D.; VanLandingham, M.; Gu, X.; Nguyen, T. *Langmuir* **2000**, *16*, 9448–9459.

(26) Raghavan, D.; Gu, X.; VanLandingham, M.; Nguyen, T. *Macromol. Symp.* **2001**, *166*, 297–305.

(23) Nyamjav, D.; Ivanisevic, A. *Adv. Mater.* **2003**, *15*, 1805–1809.

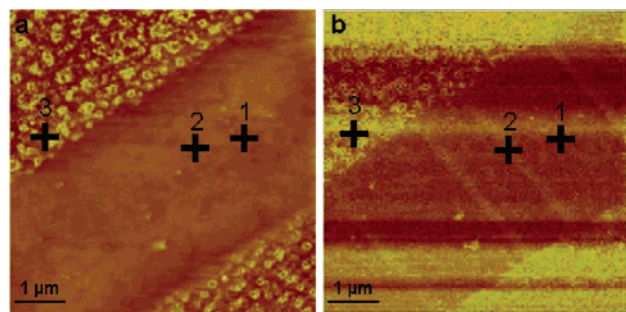


Figure 2. Topographical (a) and force volume (b) images of the template collected with a clean tip. The scan size is $6 \times 6 \mu\text{m}^2$. The color Z scale corresponds to 80 nm in (a) and 200 mV in (b). The numbers in the images (1, 2, and 3) correspond to regions that were used to construct the histograms in Figure 3 in parts (a), (b), and (c), respectively.

In this case, the phase image alone cannot be used to assign specific differences in the properties of the two types of lithographically defined features. Despite the fact that the chemical composition of both types of lithographic patterns is determined by the same ink, PAH, the differences in the phase images can also be attributed to variations in stiffness and viscoelasticity of the material²⁴ after it is delivered to and packed on the surface. From the consistency of the phase contrast one can conclude that the DPN patterns appear more homogeneous. Another imaging mode is needed to get a better understanding of the mechanical and/or chemical properties of the template.

Force volume (FV) imaging was used to gain further insight into the properties of the generated template, Figure 2. In this mode, force curves are collected at each pixel of the image. Information with respect to the adhesion between the tip and the sample can be calculated from the numerous force curves collected. An additional advantage of this mode is that height and FV images are collected simultaneously. In our experiments, FV images were collected at a Z travel distance of 50 nm with a sample number of 16 points per force curve. For every experiment 128 sample points per line were obtained. A trigger threshold of 0.01 V was used to eliminate the system's drift. The topography images were collected simultaneously at 256 sample points per line. A similar approach has been used to assess adhesion properties of single-walled carbon nanotubes through FV imaging.³⁰ The topography image collected in this mode, Figure 2A, showed 1–2-nm-high PAH stripes fabricated by microcontact printing. In this image one cannot distinguish any of the patterns generated by DPN. However, the FV image collected at the same time, Figure 2B, reveals both types of patterns with the thinner lines going diagonally across the image being the DPN features. Figure 3 shows the distribution of adhesion forces on the various parts of the surface generated by microcontact printing and DPN. We used a single FV image and extracted force curves from different regions to construct the histograms shown in

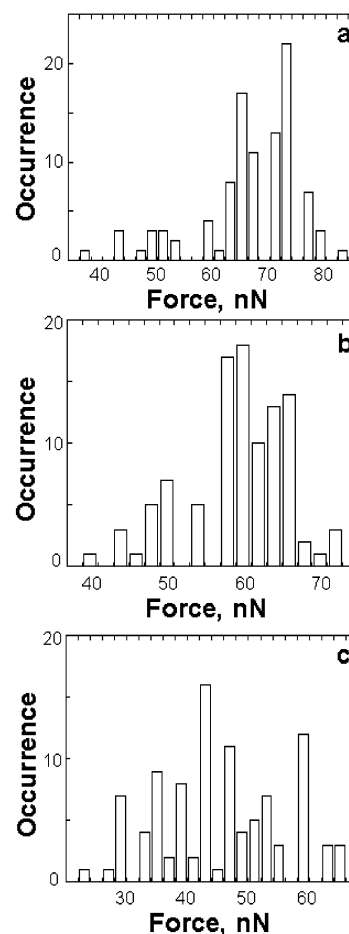


Figure 3. Histograms showing the distribution of forces required to separate a clean cantilever from (a) a clean SiO_x surface, (b) a surface patterned with PAH via DPN, and (c) a surface patterned with PAH via microcontact printing.

Figure 3. The arithmetic means and standard deviations we obtained from the histograms were 66.6 ± 8.8 nN, 58.4 ± 6.8 nN, and 46.0 ± 10.5 nN for areas in the image corresponding to clean SiO_x surfaces, patterns generated by DPN, and patterns generated by microcontact printing, respectively. Since the data were extracted from a single FV image and were collected with one tip, one can directly compare the interaction between the clean tip and various regions. Since our experiments were done in air, the FV image gives information regarding differences in hydrophobicity of the structures on the surface.³¹ This type of analysis has been used to monitor changes in the surface chemistry of substrates as they undergo reactions.³² As a comparison among the various regions on the surface one can view the microcontact-printed patterns as less hydrophilic than the rest of the surface. Furthermore, based on the arithmetic means we extracted from the histograms shown in Figure 3, the relative hydrophilicity of the regions on the surface is $\text{SiO}_x > \text{DPN-generated PAH patterns} > \text{microcontact-printed PAH patterns}$. The proof-of-concept imaging experiment we report in this paper does not allow us to account for differences in the chemical or charged nature of different parts of the template. However, in future

(27) Bar, G.; Thomann, Y.; Brandsch, R.; Cantow, H. J. *Langmuir* **1997**, *13*, 3807–3812.

(28) Bar, G.; Thomann, Y.; Whangbo, M. H. *Langmuir* **1998**, *14*, 1219–1226.

(29) Sauer, B. B.; McLean, R. S.; Thomas, R. R. *Langmuir* **1998**, *14*, 3045–3051.

(30) Poggi, M. A.; Bottomley, L. A.; Lillehei, P. T. *Nano Lett.* **2004**, *4*, 61–64.

(31) vanderWerf, K. O.; Putman, C. A. J.; deGroot, B. G.; Greve, J. *Appl. Phys. Lett.* **1994**, *65*, 1195–1197.

(32) Grinevich, O.; Mejiritski, A.; Neckers, D. C. *Langmuir* **1999**, *15*, 2077–2079.

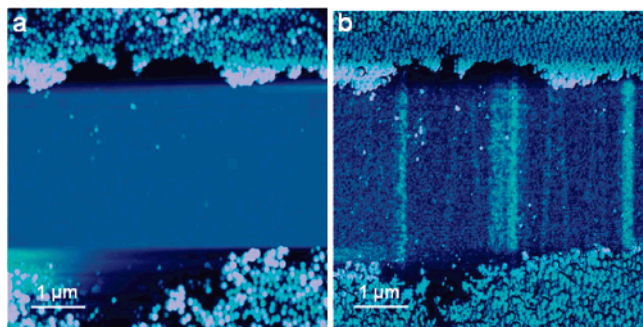


Figure 4. TMAFM images of a template surface composed of PAH patterns generated by DPN and microcontact printing after exposure to a colloidal solution as described in the text. These TMAFM images were acquired simultaneously with a scan size of $5.6 \times 5.6 \mu\text{m}^2$ and a frequency of 1.197 Hz. The height scale in (a) is 250 nm and in (b) is 60° of phase lag.

experiments we plan to utilize FV imaging in solution with tips modified with various functional groups to gain further insight into the properties of the micro- and nanostructures.

A properly engineered surface template can be used to guide or resist the assembly of molecules, colloids, or particles.^{16,17,33,34} To further compare the properties of the two types of lithographic patterns we performed a self-assembly experiment shown to be primarily governed by electrostatic interactions.³⁵ A colloidal solution of polystyrene (PS) particles (Aldrich) with a diameter of 100 nm and concentration of 12.5×10^{12} (5 wt % in water) particles/cm³ was used. The latex particles were suspended in sodium azide (0.02 wt % in water) giving each particle a net charge of $1.5 \times 10^5 e^-$ with a surface charge density of $-20 \mu\text{C}/\text{cm}^2$. The patterned substrates were exposed to the colloidal solution for 20 min to 3 h. The substrates were rinsed with DI water for 30 s followed by drying with nitrogen. Images collected by TMAFM, Figure 4, show that colloids adsorb only onto the microcontact-printed patterns. Other researchers have reported colloidal adsorption experiments on microcontact-printed patterns composed of polyelectrolytes and have observed the directed placement of properly charged colloids.¹⁶ We recorded increased packing of colloids onto the microcontact-printed patterns only after longer incubation times, and, at the same time, no consistent assembly onto the DPN patterns was observed regardless of the pattern size. Although there are many factors that can contribute to this selective assembly in addition to surface roughness,³⁶ we believe that the governing factor is the variable surface charge density of the two types of patterns. Our previous studies have shown that the DPN patterns composed of PAH can be used to guide the placement of charged DNA molecules.²³ To test whether significantly smaller particles will attach to the DPN- and microcontact-printed patterns we used small charged magnetic particles prepared by a literature procedure reported by Fu et al.³⁷ The diameter of these particles ranged

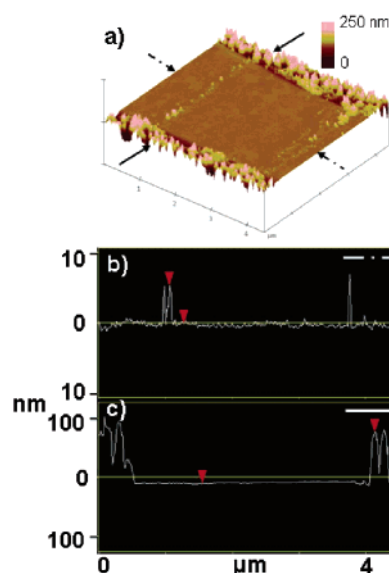


Figure 5. (a) 3D AFM topography image collected after the sequential adsorption of PS and magnetic particles. Parts (b) and (c) represent the line profiles indicated by the arrows in (a).

from 2 to 10 nm. The template containing patterns generated by DPN and microcontact printing was sequentially exposed to PS particles and magnetic nanoparticles. The results of this experiment are shown in Figure 5. While we observed that the smaller particles did adsorb onto the DPN patterns they also attached to the microcontact-printed regions that were not fully covered with the PS particles. This experiment supports our hypothesis that the variable surface charge helps the selective adsorption of certain types of particles onto parts of the template. Future studies with a variety of nanoparticle sizes and different types of polyelectrolytes can help us determine how to better control this process. These experiments are underway in our laboratory.

In summary, this study describes the following: (1) a methodology that combines the layer-by-layer approach with DPN and microcontact printing; (2) a way to map the mechanical properties of the two types of structures on the same surface through FV imaging; (3) a set of experiments that show differences in the surface chemistry between patterns generated by microcontact printing and DPN; and (4) a comparison between the selectivity of particle adsorption onto both types of lithographic patterns. The template we fabricate in this study opens new possibilities to test and compare the selective deposition of multiple types of particles, biomolecules, and cells on the same surface. Such studies can be used to address important questions with respect to cell adhesion behavior using a flexible and low-cost approach.

Acknowledgment. This material is based upon work supported by NASA under award NCC 2-1363. Any opinions, findings, and conclusions or recommendations expressed in this material are those of the authors and do not necessarily reflect the views of the National Aeronautics and Space Administration. CM049179T

(33) Zheng, H.; Rubner, M. F.; Hammond, P. T. *Langmuir* **2002**, *18*, 4505–4510.

(34) Vazquez, E.; Dewitt, D. M.; Hammond, P. T.; Lynn, D. M. *J. Am. Chem. Soc.* **2002**, *124*, 13992–13993.

(35) Chen, K. M.; Jiang, X.; Kimerling, L. C.; Hammond, P. T. *Langmuir* **2000**, *16*, 7825–7834.

(36) Clark, S. L.; Hammond, P. T. *Langmuir* **2000**, *16*, 10206–10214.

(37) Fu, L.; Dravid, V. P.; Johnson, D. L. *Appl. Surf. Sci.* **2001**, *181*, 173–178.